Journal of Power Sources 269 (2014) 363–369

Contents lists available at ScienceDirect

Journal of Power Sources

journal homepage: www.elsevier.com/locate/jpowsour

Controlling for peak power extraction from microbial fuel cells can increase stack voltage and avoid cell reversal

Hitesh C. Boghani [a], George Papaharalabos [b], Iain Michie [a], Katrin R. Fradler [a], Richard M. Dinsdale [a], Alan J. Guwy [a], Ioannis Ieropoulos [b, 1], John Greenman [b], Giuliano C. Premier [a, *]

[a] Sustainable Environment Research Centre (SERC), Faculty of Computing, Engineering and Science, University of South Wales, Llantwit Rd, Pontypridd, Mid-Glamorgan CF37 1DL, UK
[b] Bristol Robotics Laboratory, University of the West of England and University of Bristol, Bristol BS16 1QY, UK

HIGHLIGHTS

- It is possible to avoid voltage reversal in stacked MFCs despite feed imbalance.
- We applied MPPT along with hybrid connectivity to prevent voltage reversal.
- MPPT improved stack performance compared to series/parallel connectivity alone.
- The strategy is transferable between significantly different MFC systems.

GRAPHICAL ABSTRACT

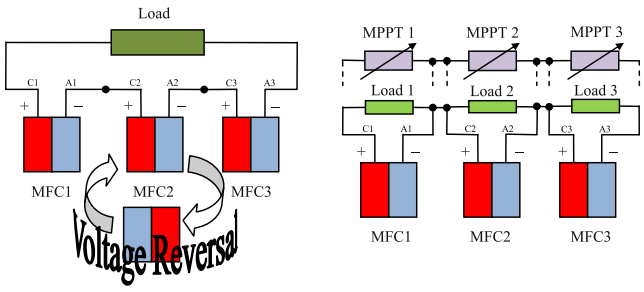

ARTICLE INFO

Article history:
Received 20 March 2014
Received in revised form
3 June 2014
Accepted 11 June 2014
Available online 7 July 2014

Keywords:
Microbial fuel cells
Cell reversal
Maximum peak power point tracking
MFC stacks
Urine
Transferability

ABSTRACT

Microbial fuel cells (MFCs) are bioelectrochemical systems which can degrade organic materials and are increasingly seen as potential contributors to low carbon technologies, particularly in energy recovery from and treatment of wastewaters. The theoretical maximum open circuit voltage from MFCs lies in the region of 1.1 V, but is reduced substantially by overvoltage losses. Practical use of the power requires stacking or other means to increase voltage. Series stacking of MFCs with typically encountered variability in operating conditions and performance raises the risk of cell reversal, which diminishes overall power performance. A novel strategy of MFC subsystem series connectivity along with maximum power point tracking (MPPT) generates increased power from individual MFCs whilst eliminating cell reversal. MFCs fed with lower concentrations of substrate experienced voltage reversal when connected in normal series connection with one common load, but when MFCs and loads together were connected in series, the underperforming cell is effectively bypassed and maximum power is made available. It is concluded that stack voltage may be increased and cell reversal avoided using the hybrid connectivity along with MPPT. This approach may be suitable for stacked MFC operations in the event that large scale arrays/modules are deployed in treating real wastewaters.

1. Introduction

Microbial fuel cells (MFCs) are a promising technology, capable of generating electricity whilst degrading/oxidising organic substances such as food processing wastes, at their anodes. Such COD

* Corresponding author. Tel.: +44 (0)1443 482333; fax: +44 (0)1443 482169.
E-mail addresses: ioannis.ieropoulos@brl.ac.uk (I. Ieropoulos), iano.premier@southwales.ac.uk (G.C. Premier).
[1] Tel.: +44 (0) 1173286318; fax: +44 (0) 1173283960.

http://dx.doi.org/10.1016/j.jpowsour.2014.06.059
0378-7753/

removal is catalysed by electrogenic bacteria, which use the anode as an electron acceptor and produce a current flow with the aid of (typically) an oxygen reduction reaction at the cathode electrode. Although these bioelectrochemical devices can develop theoretical open circuit voltages of 1.1 V (at NTP, pH 7 and acetate concentration of 5 mM) [1], the highest open circuit voltages achieved are *circa* 0.8 V. When operated under load, MFCs are able to generate working voltages of approximately 0.5 V [2].

The voltage generated from individual MFCs is insufficient for most practical applications such as powering electronics or charging batteries, and so they would benefit from stacking in series to increase the voltage. Many researchers have stacked MFCs in this way e.g. Aelterman et al. [3] stacked 6 individual MFCs to boost the voltage and were able to persistently extract power. But at high current levels, towards the maximum power available from the MFCs, the voltage from some of the MFCs diverged and reversed. This cell reversal behaviour has been observed by several researchers, as in the work of Taniguchi et al. [4] whilst investigating proton exchange membrane (PEM) fuel cells. They attributed the cause of this cell reversal to fuel starvation, including during start-up. Oh and Logan [5] confirmed that fuel starvation could have the same effect in MFC systems. Cell reversal should be avoided as it causes serially connected stacks of MFCs to underperform, as power is lost within the stack in sustaining the voltage of the reversed cell(s). When serially wired, MFCs should be operating with similar and sufficient substrate concentration, whilst having fully enriched electrogenic biofilms on their anodes and with active cathodes, they may thus be expected to produce comparable electrical and ionic currents to each other and voltage reversal should not occur during the stack operation [6]. An imbalance in the organic strength of substrate supplied to stacked MFC cells is likely to occur in practice and in circumstances where volumetric throughput is important, such as in wastewater treatment applications; it is even more likely as MFCs will tend to be hydraulically connected in series and substrate will be progressively consumed as it passes through the system [6–8].

Application of a bank of capacitors for charge accumulation from MFCs electrically connected in series has allowed energy harvesting from MFCs to perform useful tasks as evidenced in Ref. [9]. Kim et al. [2] demonstrated that cell reversal could be avoided by providing a bank of capacitors arrangement in such a way that they would be charged by MFCs connected in parallel and then discharged simultaneously in series across a load. However, the impedance of an MFC varies with changes in substrate concentration, operating temperature, buffer concentration, pH, biofilm ecology and structure, all of which might be expected to dynamically vary during reactor operation [10–12] e.g. wastewater treatment. The state of the system is therefore seldom likely to be static. An MFC could be operated to match its real-time impedance as in Refs. [13,14], which could be coupled to the charging and discharging of capacitors by suitable control of current sourcing. Therefore, we present a novel study which seeks to determine if controlling the current sourced from individual MFCs whilst simultaneously connected in series can avoid cell reversal and maximise the power they generate.

2. Materials and methods

2.1. Tubular MFC (t-MFC) construction and operation

Three independent tubular MFCs (t-MFC1, t-MFC2 and t-MFC3) with approx. 220 mL anodic volume were constructed and enriched, as previously described [15] and operated in a temperature controlled chamber at 30 ± 2 °C with 40 mM acetate in their anodes. Polarisation curves were determined for the t-MFCs by stepwise reducing the electrical load from 5 kΩ to 5 Ω using a resistor box and power was normalised to the empty bed volume of the anode.

When beginning each set of experiments, t-MFC1 and t-MFC3 were provided with 2 mM sodium acetate as substrate whereas t-MFC2 was fed 0.5 mM sodium acetate unless otherwise specified, to instigate substrate imbalance, which is plausible in practice. Substrate was provided with 50 mM phosphate buffer and nutrients as previously described [15]. All t-MFCs were operated in batch mode at ambient temperatures of 30 ± 2 °C according to the experimental set-up elaborated below and until the substrate was apparently depleted.

CASE-1: The MFCs were connected in series, connecting anodes to cathodes. The stack of MFCs was connected to a static load of 150 Ω as shown in Fig. 1a.
CASE-2: Each MFC was connected to the maximum power point load of 50 Ω (static) determined a *priori* using power curves (power *vs.* current). The MFCs and associated loads were then connected in series as shown in Fig. 1b. During CASE-1 and CASE-2 experiments, the voltage drop across the individual MFC loads and the stack voltage was sampled at 30 s intervals using a PC equipped with LabVIEW™ and NI USB-6218 (National Instruments, Newbury, UK).
CASE-3: As shown in Fig. 1c, each MFC was connected to a maximum power point tracking (MPPT) device which controlled the current sourced from each MFC. Boolean logic based hill climbing control [16] was implemented by varying the load in response to the gradient of the power curve and of its rate of change. Additionally, logic increased the load in steps *if* (conditional) MFC voltage < 0.1 V. A digital potentiometer (Intersil® X9C102, Farnell UK Ltd., Leeds) was used as the load to control the current *via* a PC equipped with LabVIEW™ and NI USB-6218. The implementation of the LabVIEW™ algorithm is presented in Supplementary information S1. The current sourced from the MFCs was regulated using digital potentiometers and thus actuated the MPPT. The voltage drops across these potentiometric loads and across the entire stack were digitally sampled at intervals of 150 s.

2.2. Small-scale MFCs (s-MFCs) construction and operation

The small 6.25 mL MFCs (Fig. 5), are of a well-established MFC design in the literature [17] and were first introduced in the EcoBot-III project. It is built entirely from Nanocure RC25 terracotta resin. The internal volume of the anode is 6.25 mL with a projected surface area of 20 mm × 30 mm and the cathode is open-to-air. s-MFCs were operated at ambient temperature (22 ± 3 °C) and supplied with fresh urine. Polarisation curves were determined for the s-MFCs in a similar manner to that for the t-MFCs, with loads ranging from 30 kΩ to 4 Ω.

s-MFC1 and s-MFC3 were fed with neat urine (as organic substrate) and s-MFC2 was provided with 1:1 diluted urine with distilled water. s-MFCs were connected in the same configuration as the experiments employing t-MFCs. However, in CASE-1 a static load of 8 kΩ was used to match the overall internal resistance of the s-MFCs; In CASE-2, static loads of 2 kΩ were used for s-MFC1 and s-MFC3, and 4 kΩ static load for s-MFC2 and; In CASE-3, a digital potentiometer (Intersil® X9C103, Farnell UK Ltd., Leeds) was used such that it suited the range of current evident from the power curve obtained from the s-MFCs.

2.3. Prolonged voltage reversal and its effect on biofilms/ecology

Acetate concentrations of 0.5 mM (t-MFC1), 0.5 mM (t-MFC2) and 2 mM (t-MFC3) were respectively fed in batch to each of the t-

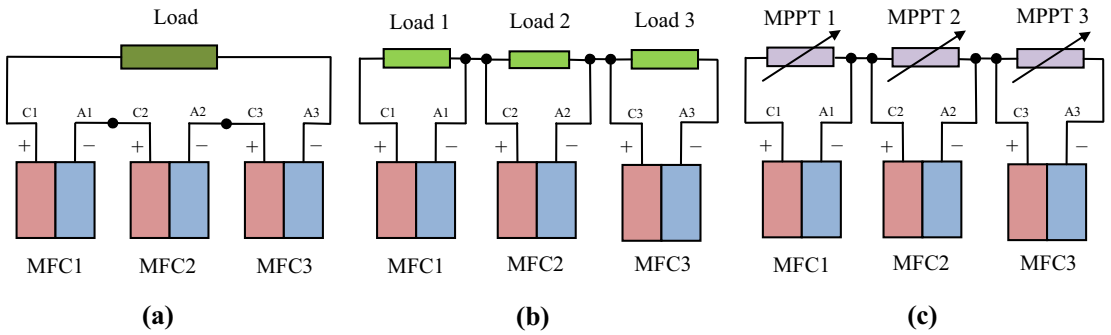

Fig. 1. (a) MFCs connected in series across an overall load of 150 Ω (unless otherwise specified) to match the collective internal resistance, CASE-1. (b) MFCs connected to the loads individually, matching their individual internal resistances, CASE-2; and (c) connected to MPPTs individually which are then connected in series, CASE-3.

MFCs, which were connected separately to a static load of 70 Ω until the substrate was depleted. The results were considered as a control experiment for this paper. It can be noted that the individual maximum power points of all t-MFCs had shifted from 50 Ω to 70 Ω by this time. To investigate the effect of prolonged voltage reversal on the anodic biofilm, the t-MFCs were given the same concentrations of acetate as previously and they were electrically connected in series with an overall stack load of 210 Ω to match the combined internal impedances of the three t-MFCs. Liquid and biofilm samples were collected when the substrate was added and when the substrate had depleted.

2.4. Ecological analysis of the anodic biofilm

Biofilms were analysed at the start and end of the prolonged voltage reversal experiment after the t-MFC2 reactor was observed to have undergone cell reversal in CASE-1. The influence of cell reversal on the anodic microbial ecology was then investigated.

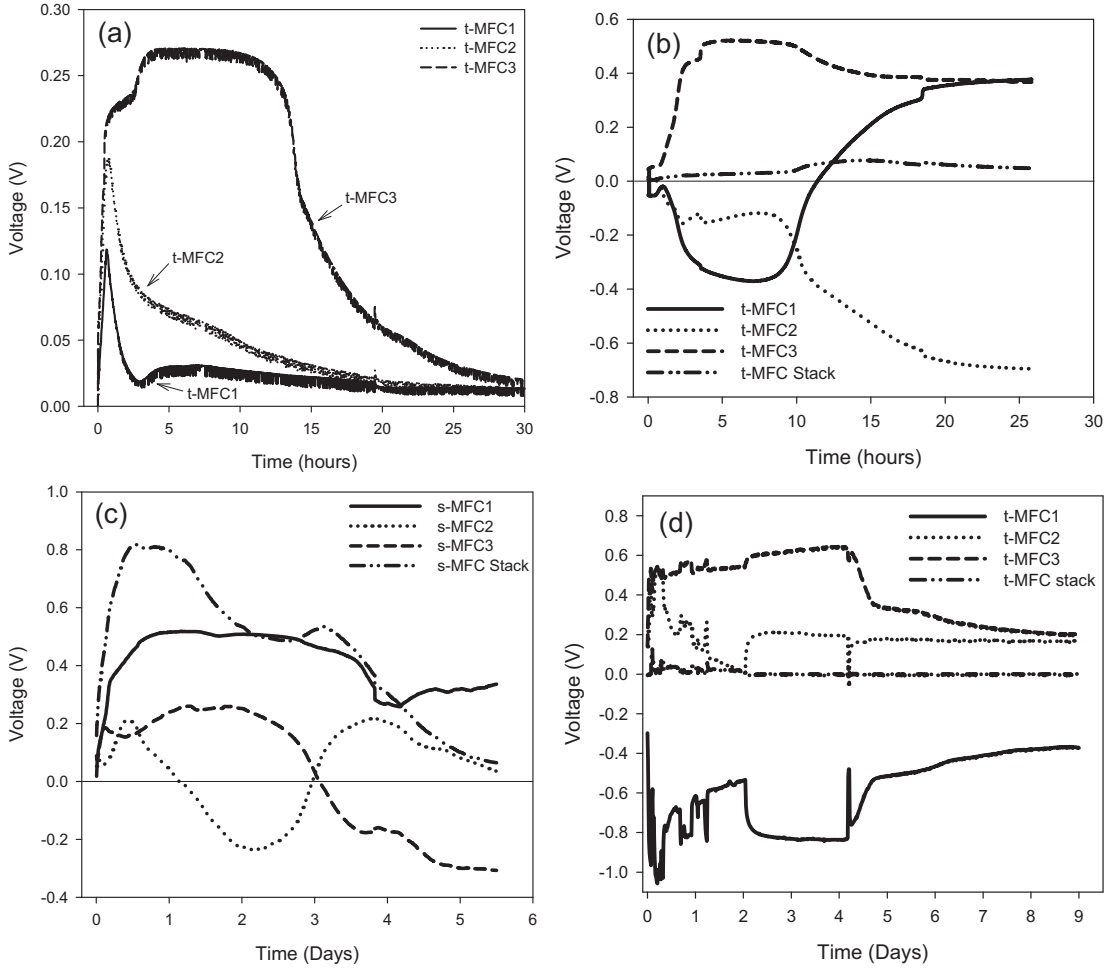

Fig. 2. (a) Voltage across 70 Ω loads that were connected to t-MFCs which were electrically independent, as a control with t-MFC1, t-MFC2 and t-MFC3 fed with 0.5 mM, 0.5 mM and 2 mM Sodium acetate respectively. Voltages across MFCs in series and overall stack voltage across an overall static load as in CASE-1 for (b) t-MFCs with stack load of 150 Ω; and (c) s-MFCs with stack load of 8 kΩ and (d) t-MFCs with stack load of 210 Ω.

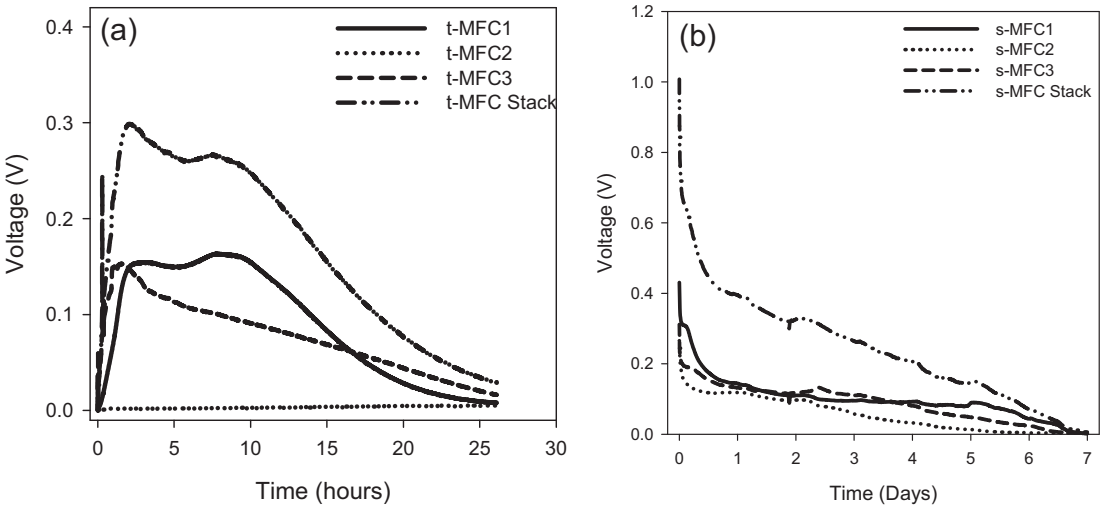

Fig. 3. Voltage across static loads on individual MFCs and overall stack voltage as in CASE-2 for (a) t-MFCs; and (b) s-MFCs.

Biofilm samples were collected by aseptically cutting a 1 cm^2 square portion of the carbon veil anode, the samples were then stored at −80 °C before processing.

The PCR Amplification of rDNA (16S rDNA) was performed as previously described [18] using the Universal bacterial primers 0109F-T and 0515R-GC (forward primer 5′-CGC CCG GGG CGC GCC CCG GGC GGG GCG GGG GCA CGG GGG G ATC GTA TTA CCG CGG CTG CTG GCA C-3′ and reverse primer 5′-ACT GCT CAG TAA CAC GT-3′). A D-Count system (Bio-Rad, Hercules, CA, USA) was used to carry out the DGGE analysis using 20%–80% denaturing gradient (100% denaturant consisting of 7 M urea and 40% (v/v) formamide) in the 8% (w/v) polyacrylamide gels. Microbial ecological analysis of the DGGE gels was carried out using GelCompar II software (Applied Maths, Belgium). Hierarchical clustering analysis utilized the Dice Index of Similarity method as a band based nearest-neighbour correlation and UPGMA (average linking method).

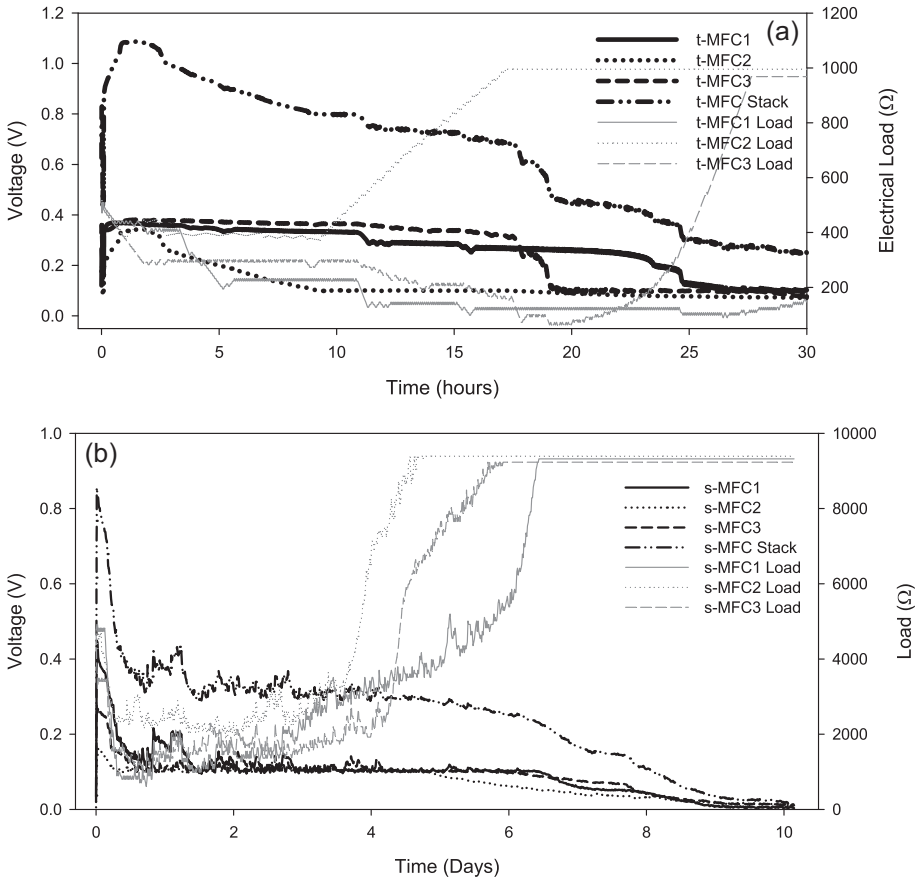

Fig. 4. Voltage across MPPT loads on individual MFCs and overall stack voltage as in CASE-3 for (a) t-MFCs; and (b) s-MFCs.

Fig. 5. DGGE bacterial community profiles from t-MFC1, t-MFC2 and t-MFC3. Cluster analysis was carried out using the Jaccard coefficient of similarity measurement.

3. Results

The results obtained from experiments CASE-1, CASE-2 and CASE-3 are shown in Figs. 2–4 , respectively. Since, these experiments (CASE-1, CASE-2 and CASE-3) were carried out on two different MFC systems with differences in scale (anodic volumes of 220 mL *vs*. 6.25 mL) and substrate (acetate *vs*. urine), the experiment was demonstrated to be transferable and showed that similar trends in results were observable. Duplicated results from t-MFCs and s-MFCs for each of CASE-1, CASE-2 and CASE-3 are presented in Supplementary information S2, from which it can be seen that the general trend is maintained, hence leading to similar conclusions.

3.1. MFC power generation

The maximum power levels determined from power curves derived from t-MFC1, t-MFC2 and t-MFC3 were 4.0, 4.0 and 4.6 W m^{-3} (anodic volume), respectively; all occurred at 50 Ω external load (40 mM sodium acetate) before executing CASE-1, CASE-2 and CASE-3 experiments, but subsequently increased to 70 Ω.

Similarly, the s-MFCs were tested according to CASE-1, CASE-2 and CASE-3 and the maximum power levels from s-MFC1, s-MFC2 and s-MFC3 were determined to be 7.7, 4.6 and 8.4 W m^{-3} (anodic volume) and occurred at external loads of 2 kΩ, 4 kΩ and 2 kΩ, respectively.

3.2. MFC voltage reversal

Fig. 2a shows that after the addition of substrate, the t-MFCs can be seen to respond as the voltage develops to a steady-state value, up until the substrate starts to deplete and the voltage can be observed to decay. As shown in Fig. 2b, after the addition of substrate to the anode according to CASE-1, t-MFC3 started-up and the voltage developed to 0.5 V within 5 h. However, the voltage of t-MFC2 reversed as a result of the lower substrate concentration. t-MFC1 started-up less rapidly, resulting in a stack voltage of <0.1 V. After 9 h, t-MFC1 developed a positive cell voltage, recovering fully after 20 h, but t-MFC2 was severely affected, causing a cell reversal voltage of −0.7 V.

The s-MFCs responded similarly to the addition of substrate very rapidly and developed voltages as per their normal performance (Fig. 2c). However, the voltage of s-MFC1 reversed after 1 day of operation in series, recovering on day 3 and at the same time s-MFC3 reversed indicating a cell voltage of −0.3 V by day 5.5 approx. Duplicate results presented in Supplementary information S2, show reversal and similar voltage trends when considered within the context of microbially catalysed systems.

Fig. 2d shows the voltage levels across the t-MFCs, where t-MFC1 and t-MFC2 were fed lower concentrations (0.5 mM) of substrate than t-MFC3 (2 mM) and the overall stack external load was 210 Ω. The stack was subsequently left in this condition for a significantly extended period (9 days in comparison to 1 day approx) in order to provide sufficient time to discern the effects of voltage reversal on the biofilm. It can be seen that the voltage remained reversed in t-MFC1 for the whole 9 day duration. The temporal development of the voltage of t-MFC1 can be seen to correlate with and reflect that of t-MFC2 up to day 4.2 in Fig. 2d, and then appeared to reflect the trajectory of t-MFC3 up to day 9. However, the overall stack voltage remained below 0.1 V for most of the 9 days presented in Fig. 2d.

Notably, in CASE-2 (Fig. 3a) it can be seen that none of the MFCs exhibited cell reversal, despite t-MFC1 and t-MFC3 being able to generate only *circa* 0.15 V t-MFC2 was evidently not able to start, generating a maximum stack voltage of *circa* 0.3 V only. As in CASE-2, when s-MFCs were connected to their respective loads, the voltage drop across the load was 0.4 V immediately, but it dropped to approx. 0.2 V by hour 12, continuing to gradually decrease until day 7 as the substrate depleted (Fig. 3b).

In CASE-3, the initial electrical MPPT loads for all t-MFCs and s-MFCs were selected to be 500 Ω (Fig. 4a) and 4.7 kΩ, respectively. The MPPT system was able to track the maximum power point from measures of the MFCs' individual voltages. All three t-MFCs were able to start-up within 2 h and generated individual voltages between 0.3 and 0.4 V; with overall stack voltages of up to 1.1 V over this period as seen from Fig. 4a. However, t-MFC2's voltage started dropping, resulting in an increased external load being applied by the MPPT control strategy, in order to avoid reversal of cell voltage. This was also observed in t-MFC1 and t-MFC3 when substrate depletion became evident. Also, in the case of s-MFCs (Fig. 4b), the MPPT loads tracked the maximum power and the individual voltages were approximately 0.1 V before substrate depletion became a dominant factor. Lack of substrate is evidenced through the dropping cell voltage and increasing external load where t-MFC2 load and s-MFC2 load started increasing first as compared to the MFC1 and MFC3 reactors, confirming comparatively less substrate was available in t-MFC2 and s-MFC2. The data shown in Figs. 3b and 4b have been reduced by re-sampling at 15 min intervals for the sake of presentation clarity. However, the procedure did not alter the information content of the data in respect of the observations and conclusions drawn. Electrical current and power are omitted for clarity in favour of voltage, but may be determined from the electrical loads and voltages. However, current and power generation from t-MFCs and s-MFCs are shown for the duplicate results in Supplementary information S2 for CASE-1, CASE-2 and CASE-3.

3.3. Cluster analysis for anodic biofilm

The effect on microbial ecology of the reactor configuration and connectivity in CASE-1 was examined using DGGE analysis (Fig. 5). Operating the reactors while electrically connected in series resulted in a reversal of t-MFC2's cell voltage (Fig. 2a) and t-MFC1 (Fig. 2d). Prior to this voltage reversal, Cluster analysis showed that all 3 reactors had similarity scores of >90%. After the voltage reversal, it was found that only t-MFC1 and t-MFC3 reactors had a similarity score of 92.3%, with the score of t-MFC2 reducing to 83.3%.

4. Discussion

Fig. 2a shows voltage profiles generated by different concentrations of acetate, i.e. 0.5 mM and 2 mM. The acetate

concentrations used in the experimentation reported in this study were at sufficiently high level to produce power from the MFC(s) fed with 2 mM concentration, whilst there is a decline in power from MFC(s) fed with lower (0.5 mM) concentration (as seen from the voltage plot in Fig. 2a, after 2.5 h), operating in the stack. The reversal of cell voltage observed in CASE1 (Fig. 2b–d) is expected and in agreement with studies by others [3,5]. This is potentially a significant barrier in MFC stack operation.

4.1. Mechanism of voltage reversal

CASE-1, CASE-2 and CASE-3 scenarios were found to apply equally to both tubular and small-scale MFCs. However as an example, the tubular MFC1, MFC2 and MFC3 may be considered when supplied with 2 mM, 0.5 mM and 2 mM concentrations of acetate respectively. The voltage reversal phenomenon has been previously described in Ref. [10] by using hydraulics as an analogy. Nevertheless, voltage reversal may be considered in the context of the tubular MFC1, 2 and 3 and the cases applied to them. Anode and cathode connections are identified as A1, A2 and A3 and C1, C2, C3, respectively (Fig. 1). In CASE-1, when insufficient substrate is available to generate electric current from A2, its voltage will assume that of C3, to which it is connected. Cationic current in MFC2 will also be minimal compared to other MFCs in the stack. The cathodic reaction in MFC2 will then also largely cease. C2 will hence be unable to sink current from A1 and will assume the voltage of A1. This will result in a reversal in voltages across MFC2 (A2 and C2). MFC2 thus becomes a parasitic internal load, through which current must pass from A1 to C3. The stack voltage will be lowered as a consequence and this is clearly seen in Fig. 2b and c. Also, when 70 Ω is connected to individual t-MFCs, they do not produce more than 0.3 V (Fig. 2a) and a voltage level of more than 0.4 V and 0.5 V is produced when they are connected to a load of 1 kΩ and 5 kΩ, respectively (evident from power curve presented in the Supplementary information S2). The voltage of t-MFC3 in Fig. 2b and d appear on occasions to approach 0.5 V and 0.6 V the point where comparatively low current is flowing through an overall stack load of 150 Ω (evidenced by a voltage drop across 150 Ω of <0.1 V). This indicates that t-MFC2, unable to provide current, becomes a very high parasitic load in the circuit. A similar effect is evident in s-MFC1 in Fig. 2c.

4.2. Avoiding voltage reversal

In CASE-2 and CASE-3, the individual MFCs with their individual loads are subsequently connected in series, which appears as bridging throughout the whole stack (Fig. 1b and c). When A2 stops producing current, the electrons used in the reduction of C3 can come through the external load of MFC3 (and/or MFC2) and similarly when the cathodic reaction in MFC2 is seriously restricted by lack of cations, the electrons generated at A1 can reach C1 and C3 *via* external loads. So, in this way, the underperforming MFC can be by-passed with minimal diminution of the performance of the whole stack. This can be seen in Figs. 3 and 4 from the fact that none of the MFCs (t-MFCs and s-MFCs) exhibited voltage reversal. Furthermore, the power generation from t-MFC1 and t-MFC3 was not affected by the lower performance of t-MFC2 (after 5 h in Fig. 4a) and similarly, s-MFC2 was also producing somewhat lower power than the other s-MFCs in the stack but did not affect their performances (Fig. 3b and after day 5 in Fig. 4b).

The stack configuration shown in Fig. 3a resulted in no voltage (hence power) generation from t-MFC2 (Fig. 3), which had been fed with the lowest concentration of acetate (0.5 mM). Also, the very low voltage generated from t-MFC1 and t-MFC3 with 50 Ω loading could be due to a higher internal resistance resulting from 2 mM acetate (as opposed to 40 mM acetate during power curve measurement). However, the current sourced was not controlled as the load was fixed and so higher current was demanded, which may have rendered t-MFC2 unable to start-up.

4.3. Transferability of proposed strategy

When the MFCs (t-MFCs and s-MFCs) were connected to MPPT, the current sourced from anodophiles present in the anode, was controlled to ensure the peak power output, which would correlate to maximum COD removal. In practice, the stacking of MFCs is likely to be required and it is desirable that each MFC operates at its instantaneous peak capacity. Also, obstructions in the flow pathways could cause MFCs to receive reduced or unbalanced (cell to cell in a stack) organic loading, which if unchecked could cause temporary or permanent inactivation and cell reversal. CASE-3 demonstrates that individual MFCs could be operated at their maximum power point (Fig. 4) and the voltage could be boosted despite MFCs, electrically connected in series, not having identical substrate concentrations; so avoiding cell reversal. However, appropriate energy harvesting mechanisms are required. The t-MFCs and s-MFCs studied in this paper are significantly different from each other in terms of their architecture, substrate (fuel) type and also volumetric scale. Despite the differences, the strategy presented here, along with the MPPT, was effective in preventing cell reversal while extracting available maximum power in both designs. It is suggested that the control functionality, which would require limited memory and logic operations, could for example be implemented in appropriate ultra-low power microcontrollers, with suitable power saving functionality to require only small proportions of the MFC generated power to sustain MPPT operations (e.g. TI, MSP430™ series <100 μA/MHz; minimum 500 nA in standby mode; http://www.ti.com/lit/sg/slab034x/slab034x.pdf).

4.4. Effect on microbial ecology

The occurrence of substrate depletion and subsequent fuel cell reversal had a noticeable effect on system performance and this was also reflected by the change in the anodic microbial ecology. However, this change was small when compared to microbial community changes reported by Lyon et al. [19], although this may also reflect the fact that the biofilm in their study had only been established for a period of 18 days. The t-MFCs on which the community study was reported here had been operating for at least 2 years. Hence, whilst voltage reversal has an adverse effect on power production it does not necessarily result in large permanent shifts in the electrogenic population.

The efficacy of electrochemically active bacterial activity was also not adversely affected, as the t-MFC2 reactor that was subject to cell reversal recovered full power after 20 h (results not shown). This would suggest that the key microbial communities were not adversely affected by a reversed anodic voltage and could recover electrogenic activity quickly. Indeed it has been reported that electrogenic biofilms are capable of bi-directional flow [20] and this has been utilized in rotatable bioelectrochemical reactor systems that undergo electrode polarity inversions.

Given that MFCs running at different levels of substrate concentration in their anode are susceptible to voltage reversal when stack operation is considered and in practice, it may be difficult to distribute substrate equally amongst cells; it is necessary to adopt a strategy or device to avoid voltage reversal in MFCs while operated in stacks. The strategy presented here has been shown to be transferable between substantively different MFC designs and substrates used and may be suitable for application to energy

harvesting from MFCs implemented using low power digital electronics.

5. Conclusions

Using power from MFCs deployed in practical systems will require voltages to be increased above cell voltages, which can be achieved by stacking in series, but this approach risks the occurrence of cell voltage reversals which adversely affect the whole stack. The application of MPPT and the connection strategy presented here can increase stack voltages and avoids the reversal of cell voltage, whilst also applying a control mechanism that facilitates peak power extraction from MFCs in real-time. The strategy is transferable between different designs of MFC and with different substrates.

Acknowledgements

This research was funded by the RCUK Energy Programme, SUPERGEN Biological Fuel Cell project (EP/D047943/1 and EP/H019480/1) supported by grant 68-3A75-3-150. The Energy Programme is an RCUK cross-council initiative led by EPSRC and contributed to by ESRC, NERC, BBSRC and STFC. Ioannis Ieropoulos is an EPSRC Career Acceleration Fellow (grant numbers EP/I004653/1 and EP/L002132/1). The urine work is funded by the Bill & Melinda Gates Foundation grant no. OPP1094890.

Appendix A. Supplementary data

Supplementary data related to this article can be found at http://dx.doi.org/10.1016/j.jpowsour.2014.06.059.

References

[1] B.E. Logan, B. Hamelers, R. Rozendal, U. Schröder, J. Keller, S. Freguia, P. Aelterman, W. Verstraete, K. Rabaey, Environ. Sci. Technol. 40 (2006) 5181–5192.
[2] Y. Kim, M.C. Hatzell, A.J. Hutchinson, B.E. Logan, Energy & Environ. Sci. 4 (2011) 4662–4667.
[3] P. Aelterman, K. Rabaey, H.T. Pham, N. Boon, W. Verstraete, Environ. Sci. Technol. 40 (2006) 3388–3394.
[4] A. Taniguchi, T. Akita, K. Yasuda, Y. Miyazaki, J. Power Sources 130 (2004) 42–49.
[5] S.E. Oh, B.E. Logan, J. Power Sources 167 (2007) 11–17.
[6] L. Zhuang, Y. Zheng, S. Zhou, Y. Yuan, H. Yuan, Y. Chen, Bioresour. Technol. 106 (2012) 82–88.
[7] J.R. Kim, G.C. Premier, F.R. Hawkes, J. Rodríguez, R.M. Dinsdale, A.J. Guwy, Bioresour. Technol. 101 (2010) 1190–1198.
[8] L. Zhuang, S. Zhou, Electrochem. Commun. 11 (2009) 937–940.
[9] I. Ieropoulos, C. Melhuish, J. Greenman, in: W. Banzhaf, J. Ziegler, T. Christaller, P. Dittrich, J. Kim (Eds.), Advances in Artificial Life, Springer Berlin Heidelberg, 2003, pp. 792–799.
[10] J. Greenman, I. Ieropoulos, C. Melhuish, in: N. Eliaz (Ed.), Applications of Electrochemistry and Nanotechnology in Biology and Medicine I, Springer, 2011, pp. 239–290.
[11] Z. He, F. Mansfeld, Energy & Environ. Sci. 2 (2009) 215–219.
[12] A.K. Manohar, O. Bretschger, K.H. Nealson, F. Mansfeld, Bioelectrochemistry 72 (2008) 149–154.
[13] G.C. Premier, J.R. Kim, I. Michie, R.M. Dinsdale, A.J. Guwy, J. Power Sources 196 (2011) 2013–2019.
[14] L. Woodward, B. Tartakovsky, M. Perrier, B. Srinivasan, Biotechnol. Prog. 25 (2009) 676–682.
[15] J.R. Kim, G.C. Premier, F.R. Hawkes, R.M. Dinsdale, A.J. Guwy, J. Power Sources 187 (2009) 393–399.
[16] H.C. Boghani, J.R. Kim, R.M. Dinsdale, A.J. Guwy, G.C. Premier, Bioresour. Technol. 140 (2013) 277–285.
[17] I. Ieropoulos, J. Greenman, C. Melhuish, I. Horsfield, in: H. Fellermann, M. Dorr, M. Hanczyc, L. Laursen, S. Maurer, D. Merkle (Eds.), Alife XII Conference, MIT Press, Odense, Denmark, 2010, pp. 733–740.
[18] I.S. Michie, J.R. Kim, R.M. Dinsdale, A.J. Guwy, G.C. Premier, Energy & Environ. Sci. 4 (2011) 1011–1019.
[19] D.Y. Lyon, F. Buret, T.M. Vogel, J.-M. Monier, Bioelectrochemistry 78 (2010) 2–7.
[20] K.Y. Cheng, G. Ho, R. Cord-Ruwisch, Environ. Sci. Technol. 45 (2010) 796–802.